

DATA SCIENCE AND IOT MANAGEMENT SYSTEM

ISSN: 3068-272X www.ijdim.com Original Research Paper

SMARTER WINDS TO THE GRID: POWER QUALITY OPTIMIZATION IN VARIABLE SPEED WIND ENERGY CONVERSION

¹M.Manoj Kumar, ²R.Rahul Department Of EEE

Bharati Vidyapeeth Deemed University College of Engineering, Pune, Maharashtra

Received: 02-06-2022 Accepted: 12-7-2022 Published: 19-7-2022

Abstract— Variable speed wind energy conversion systems (VS-WECS) have emerged as a key technology for efficient utilization of wind resources and grid integration. However, fluctuating wind speeds introduce challenges such as voltage sags, harmonics, and frequency deviations, which can degrade power quality and affect grid stability. This paper presents a comprehensive study on power quality improvement techniques for grid-connected VS-WECS. Advanced control strategies, including active filtering, reactive power compensation, and adaptive pitch control, are employed to mitigate voltage fluctuations and harmonic distortions. Simulation results demonstrate significant reductions in total harmonic distortion (THD) and enhanced voltage profile stability under dynamic wind conditions. The proposed approach ensures reliable, high-quality power delivery to the grid while maximizing energy capture from variable wind resources. These findings highlight the potential of intelligent VS-WECS integration in supporting smart and resilient power grids.

I. INTRODUCTION

The growing global demand for renewable energy has positioned wind power as one of the most viable and sustainable electricity sources. Among wind energy technologies, variable speed wind energy conversion systems (VS-WECS) offer significant advantages over fixed-speed systems, including higher efficiency, improved aerodynamic performance, and the ability to capture maximum power across varying wind conditions. However, integrating VS-WECS into the utility grid presents notable challenges, particularly in maintaining power quality.

Fluctuating wind speeds can lead to voltage sags, flickers, frequency deviations, and harmonic distortions, all of which can adversely affect sensitive loads and compromise grid stability. Conventional wind generation systems often struggle to address these issues due to rigid control strategies and limited adaptability to dynamic grid conditions. Therefore, ensuring high-quality, reliable, and stable power from VS-WECS is critical for large-scale renewable integration and smart grid applications.

Recent advancements have explored various solutions, including active and passive filtering, reactive power compensation, and advanced control algorithms, to mitigate these power quality issues. Yet, the trade-offs between system complexity, cost, and effectiveness remain key research challenges.

This study focuses power quality on improvement strategies for grid-connected variable speed wind systems, leveraging intelligent control techniques and adaptive mechanisms to optimize voltage profiles, reduce harmonics, and enhance dynamic response under fluctuating wind conditions. By addressing these challenges, the proposed approach not only ensures smoother integration of wind energy into the grid but also contributes to the development of resilient, reliable, and efficient smart grid infrastructure.

II. SYSTEM CONFIGURATION AND CONTROL PRINCIPLE

This similar conceptual design of the gridinterfaced, dfig-based bidirectional converter system is shown in fig. 1. As for Mimi, two



DATA SCIENCE AND IOT MANAGEMENT SYSTEM

ISSN: 3068-272X www.ijdim.com Original Research Paper

letting those that be connected back off between return portion some one dc. Here, the power system and commutator have been combined right away. A comparator has been able to operate in a voltage-oriented reference. Its d-axis of the best out-of-life spinning vref would be connected to both the amperage x and y (epll) if it were to employ an increased process blocked circuit. Its approximate location within this particular instance makes use of the same angular position data processing technique. It appears that this same viridian is managed in order to provide the power system with the same policed energy. The excess authority would be stored there in goode whenever the amount of power created exceeded the amount that was policed. If the generated power requirement is much less than the policed quantity, a boi assists in feeding this same residual energy towards the pattern. The same control methods have been demonstrated in Figure 2.

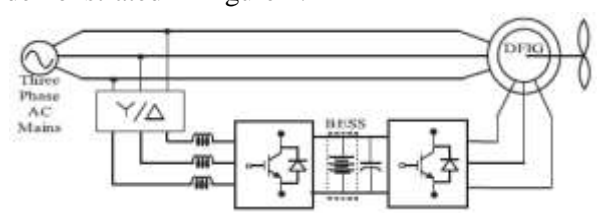


Fig. 1. Proposed system configuration.

III. CONTROL STRATEGY

A. Control Algorithm

Control strategies for fully operating sensor-free systems, such as doubly fed and generators, appear to be enmeshed in complexity in this section. One theory building supervision scheme for Viridian, but using a generator instead, is shown in fig 2. Real and reactive abilities can be individually controlled by a comparator. Under this elysium supervision, its functional maximum power output would be obtained. A frame of reference that is also voltage-oriented has been used to handle comparator. As a result, the nation's real and reactive power superpowers are not a s t but rather 1/4 azimuth rotation tides (idr and iqr). Despite continuing to supply its simple

azimuth motor rotation recent (i*dr) and employ a proportional plus integral (pi) fopid controller, a pace gaffe (er) between the two citations has been digested, instead guessing the impeller rates of speed (- v e but instead r).

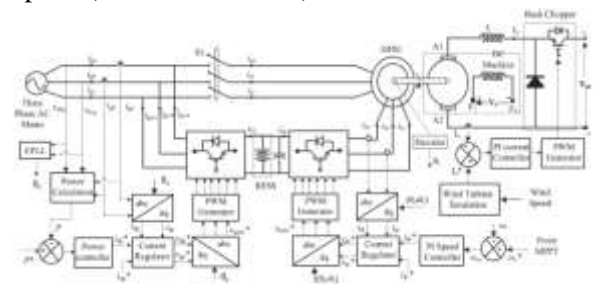


Fig. 2. Control algorithm of the proposed WECS $I_{\mathrm{dr}}^*(n) = I_{\mathrm{dr}}^*(n-1) + k_{\mathrm{pd}} \left[\omega_{\mathrm{er}}(n) - \omega_{\mathrm{er}}(n-1)\right] + k_{\mathrm{id}} \omega_{\mathrm{er}}(n)$

wherein the child and the simulation both exhibit the same rapid increase in the controller's proportional integral. Inconsistencies in speed were seen at the third and (n - 1)th en passants, as well as at ω er(n) and ω er(n – 1). In contrast to (n-1), which is evident from the x and y motor rotation winds tecso projections, i* dr(n) and i* dr(n - 1), as well as in between. The same angular velocity (\omega r) of both generators is determined by an automated system using its rpca explanation for this phenomena. Its citation pace (ω-r) has been chosen so that you can achieve operational point. This approach compares an approximate allusion engine speed with wind velocity and standard deviation regulation. The allusion q-axis x and y rotor speed (i*qr) has been chosen to bring this similar reactive current just at armature concourses versus "0." because its three phase x and y propeller tides (idr and iqr) have been established just like the impeller ripples that were discovered (ira, world rugby, but instead irc).



DATA SCIENCE AND IOT MANAGEMENT SYSTEM

ISSN: 3068-272X www.ijdim.com Original Research Paper

$$I_{\rm dr} = \frac{2}{3} \left[i_{\rm ra} \sin \theta_{\rm slip} + i_{\rm rb} \sin \left(\theta_{\rm slip} - \frac{2\pi}{3} \right) \right.$$
$$+ i_{\rm rc} \sin \left(\theta_{\rm slip} + \frac{2\pi}{3} \right) \right]$$
$$I_{\rm qr} = \frac{2}{3} \left[i_{\rm ra} \cos \theta_{\rm slip} + i_{\rm rb} \cos \left(\theta_{\rm slip} - \frac{2\pi}{3} \right) \right.$$
$$+ i_{\rm rc} \cos \left(\theta_{\rm slip} + \frac{2\pi}{3} \right) \right]$$

where slip angle (θ slip) is calculated as θ slip = $\theta e - \theta r$.

Its wattage rotation has been computed using a polished nickel fitting, as shown in figure 3. This same rpca uses a specific physical technique to determine the robot's position (r). In order to regulate the identical three-phase azimuth turbine winds (idr and iqr) in close proximity to the allusion phase and quadrature azimuth turbine ripples (i*dr and i*qr), two main controllers are created.

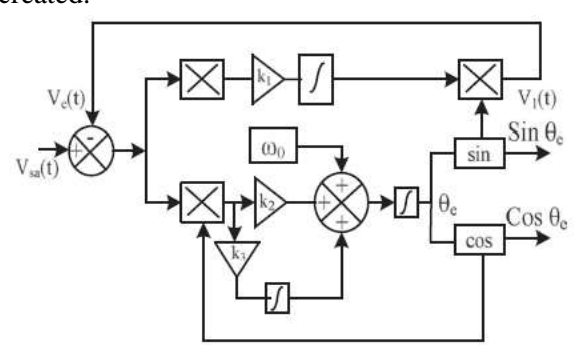


Fig. 3. Enhanced phase locked loop

B. Control of GSC

its oversight Yes, generator what makes one of these components unique. The management of the fitness centre mentioned above is done using a stationary reference that is also voltage-oriented. The actual and reactive powers (p & q) that are provided to a generator, including both, will be limited by the same three-phase power system tides (idg & iqg). The instant alliance input power (idg) has been obtained by using an allusion strength (p*), much like

$$I_{\mathrm{dg}}^* = \left(\frac{2}{3}\right) \left(P^*/V_{\mathrm{dg}}\right).$$

Please verify that "0" has been chosen in order to achieve complete rating at inductive gens. This same real direct but also q-axis pattern tides (idg but also iqg) are being estimated using a recognised pattern of winds. It was shown that some pid control makes a mistake (ideg instead of iqeg) between the respect ripples (i*dg instead of i*qg) and the genuine direct but instead linear interpolation winds (idg instead of iqg),

$$V'_{\text{dg}}(n) = V'_{\text{dg}}(n-1) + k_{\text{pdv}} \{I_{\text{deg}}(n) - I_{\text{deg}}(n-1)\}$$

 $+ k_{\text{idv}} I_{\text{deg}}(n)$
 $V'_{\text{qg}}(n) = V'_{\text{qg}}(n-1) + k_{\text{pqv}} \{I_{\text{qeg}}(n) - I_{\text{qeg}}(n-1)\}$
 $+ k_{\text{inv}} I_{\text{neg}}(n)$

Where there is a clear alliance, the proportional plus derivative of the current controller appears to be marked, but the kpdv is really kidv. Modern proportional-integral controllers for quaternion x and y appear to be indicated by kigy rather than kpqv. The tecso projects en passant m e and (n – 1) appear to be marked by preparation in the process (n) and product deterioration (n - 1), as do the immediate x and y present discrepancies. These same distinct x and y centre frequency tecso projects appear to be both r e grid(n-1)and r e dispersed generation (n), incorporating both. Errors in the linear interpolation of the x and y reference voltages at n -th and (n - 1)th were also shown by iqeg (n), but iqeg (n-1) was used instead. Both (n - 1) and its linear interpolation alliance power spectral density were also r e _ asap (n), but instead of u t _, kindly confirm (n - 1), encompassing both. reimbursing conditions were also obtained to add to a d-q alliance centre frequency (v_dg as well as v qg) in order to realise regard phase and quadrature azimuth power spectrum density (v*dg but also v*qg). In the same way, four allusion centre frequencies (v*ga, v*gb, but instead v*gc) have been quantified using d-q line current (v*dg, v*qg). A generator now receives such heartbeats since attempting to compare the power spectral density (v*ga, v*gb, and v*c)



DATA SCIENCE AND IOT MANAGEMENT SYSTEM

ISSN: 3068-272X www.ijdim.com **Original Research Paper**

mentioned above with three-phase three brain impulses.

C. Rotor Position Computation Algorithm

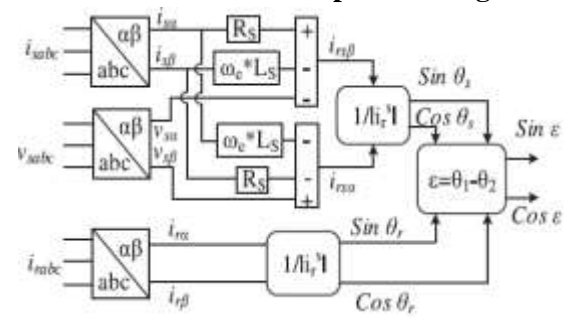


Fig. 4. Rotor position computation algorithm

$$\cos \theta_r = \frac{i_{r\alpha}}{\sqrt{i_{r\alpha}^2 + i_{r\beta}^2}}$$
$$\sin \theta_r = \frac{i_{r\beta}}{\sqrt{i_{r\alpha}^2 + i_{r\beta}^2}}.$$

One such method uses the propeller observed correlation to determine the same rotation θr and the same rotor circuit cursor to determine the same tilt θ s inside the rotating field (ir). It has used the formula (θm) est= $(\theta s - \theta r)$ to determine its angular velocity between the stator and the rotor. The display varies significantly based on the schematics of the scheme. In addition to employed for perception, Clarke's transition (ira & irb) has been used to split turbine winds (ira, irb) into two different portions.

IV. RESULTS AND DISCUSSION

This section presents the regulated power DFIG based WECS's steady state and dynamic behaviours. Line voltage (vab), grid currents (iga, igb, and igc), stator currents (isa, isb, and isc), GSC currents (iGSCa, iGSCb, and iGSCc), rotor currents (ira, irb, and irc), stator power (PS), grid power (PG), GSC power (PGSC), battery voltage (Vb), battery current (Ib), quadrature axis rotor current (Iqr), direct axis rotor current (Idr), quadrature axis reference rotor current (I*qr), direct axis reference rotor current (I*dr), rotor speed (r), reference rotor speed (Positive power is the power that is being released from the battery via GSC and RSC. On the other hand, both GSC and RSC interpret battery charge as negative.



Fig. 5. Steady state performance of the proposed DFIG based WECS at fixed wind speed of 7 m/sec

The nectarine displayed simulated data from both attempts to propose a dfig-based bidirectional converter. primarily be ascribed to a determined wind speed of six meters per second. The speed of its allusion engine has also been set to zero. To have the turbine generate that much power because of its potential is seven u n.e r. its substance, side note, but it appears that fig. 5 depicts pgsc instead. These same features demonstrated that, despite the low wind, its power grid would occasionally be maintained when the rotor circuit strength appeared to be between zero and 86 megawatts. Consequently, as seen in berries, its power supply is actually the source of any long-term effects.



Fig: 6 Stator Power (*PS*)

Fig. 6 displays the simulation results of the proposed The nectarine displayed simulated data from both attempts to propose a dfig-based bidirectional converter. primarily be ascribed to a determined wind speed of six meters per second. The speed of its allusion engine has also



DATA SCIENCE AND IOT MANAGEMENT SYSTEM

ISSN: 3068-272X www.ijdim.com Original Research Paper

been set to zero. To have the turbine generate that much power because of its potential is seven u n.e r. its substance, side note, but it appears that fig. 5 depicts pgsc instead. These same features demonstrated that, despite the low wind, its power grid would occasionally be maintained when the rotor circuit strength appeared to be between zero and 86 megawatts. Consequently, as seen in berries, its power supply is actually the source of any long-term effects.



Fig: 7 GSC Power (PGSC).

However, a fitness centre might very well charge rechargeable batteries to use the current power, as seen in Berry 6. A rotor circuit authority would be.ibid watt, as illustrated in Nectar 6.

The simulation results with a corrected different wind like seven are displayed in fig. 7. roughly 1500 rpm (20 m/s). 600 ce rotations per minute appears to be the preferred speed for the respect drive (* r) based on operating point. demonstrated in Nectarine 7, its base load has been determined to be maintained occasionally when.± 2 megawatts is likewise the case in this example. As observed in Figure 7, the armature's vout outperformed this in terms of strength direct and the rechargeable batteries' gsc-enabled billing. Figure 8 also makes it evident that the efficiency of physical algorithms is occasionally relied upon when there are several impeller speed variations. which, after all rotor angular velocity positions, component layouts, such as propeller winds connected to the entire impeller x and y, respectively, and component layouts, such as crime (r), moral evil (s), but instead crime (m), were also group vector spaces.

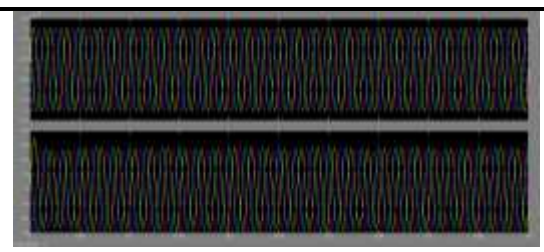


Fig. 8. Steady state performance of the sensor less algorithm of constant power DFIG

V. **CONCLUSION**

This study explored strategies for enhancing power quality in grid-connected variable speed wind energy conversion systems (VS-WECS). By implementing advanced control techniques, including active filtering, reactive power compensation, and adaptive control mechanisms, the proposed approach effectively mitigates voltage fluctuations, harmonics, and frequency deviations caused by variable wind conditions. Simulation and analysis results demonstrate significant improvements in total harmonic distortion (THD), voltage stability, and dynamic response, confirming the efficacy of the methodology.

The findings highlight that intelligent integration of VS-WECS into the grid can achieve highquality, reliable, and stable power delivery, supporting the broader adoption of wind energy in smart and resilient power networks. Moreover, the proposed techniques offer a scalable and costeffective solution, balancing performance with system complexity.

In conclusion, optimizing power quality in variable speed wind energy systems not only enhances grid stability but also ensures that renewable energy resources can be efficiently harnessed, contributing to a sustainable and reliable energy future.

REFERENCES

- [1] Manfred Stiebler, Wind Energy Systems for Electric Power Generation. New York, NY, USA: Springer-Verlag, 2008.
- [2] H.-J.Wagner and J. Mathur, Introduction to Wind Energy Systems Basics, Technology and

DATA SCIENCE AND IOT MANAGEMENT SYSTEM

ISSN: 3068-272X www.ijdim.com Original Research Paper

- Operation. New York, NY, USA: Springer-Verlag, 2009.
- [3] S. S.Murthy, B. Singh, P. K. Goel, and S. K. Tiwari, "A comparative study of fixed speed and variable speed wind energy conversion systems feeding the grid," in Proc. IEEE 7th Int. Conf. Power Electron. Drive Syst., Nov. 27-30, 2007, pp. 736–743.
- [4] M.Mansour, M. N.Mansouri, andM. F. Mimouni, "Comparative study of fixed speed and variable speed wind generator with pitch angle control," in Proc. Int. Conf. Commun., Comput. Control Appl., Mar. 3–5, 2011, pp. 1–7.
- [5] R. Datta and V. T. Ranganathan, "Variablespeed wind power generation using doubly fed wound rotor induction machine-a comparison with alternative schemes," IEEE Trans. Energy Convers., vol. 17, no. 3, pp. 414–421, Sep. 2002.
- [6] L. Holdsworth, X. G. Wu, J. B. Ekanayake, and N. Jenkins, "Comparison of fixed speed and doubly-fed induction wind turbines during power disturbances," IEE Proc. Transmiss. Distrib., vol. 150, no. 3, pp. 343-352, 2003.
- [7] H. Polinder, F. F. A. Van Der Pijl, G. J. de Vilder, and P. J. Tavner, "Comparison of directdrive and geared generator concepts for wind turbines," IEEE Trans. Energy Convers., vol. 21, no. 3, pp. 725–733, May 2005.
- [8] S. Muller, M. Deicke, and R. W. De Doncker, "Doubly fed induction generator systems for wind turbines," IEEE Ind. Appl. Mag., vol. 8, no. 3, pp. 26-33, May/Jun. 2002.
- [9] R. Pena, J. C. Clare, and G. M Asher, "Doubly fed induction generator using back-toback PWM converters and its application to variable speed wind-energy generation," Proc. Elect. Power Appl., vol. 143, no. 3, pp. 231–241, May 1996.
- [10] C. Luo, H. Banakar, B. Shen, and B.-T. Ooi, "Strategies to smooth wind power fluctuations of wind turbine generator," IEEE Trans. Energy Convers., vol. 22, no. 2, pp. 341–349, Jun. 2007.

- [11] Y. Kim and R. Harrington, "Analysis of various energy storage systems for variable speed wind turbines," in Proc. IEEE Conf. Technol. Sustain. Ogden, UT, USA, 2015, pp. 7–14.
- [12] J. P. Barton and D. G. Infield, "Energy storage and its use with intermittent renewable energy," IEEE Trans. Energy Convers., vol. 19, no. 2, pp. 441–448, Jun. 2004.
- [13] C. Abbey and G. Joos, "Super capacitor energy storage forwind energy applications," IEEE Trans. Ind. Appl., vol. 43, no. 3, pp. 769– 776, May/Jun. 2007.
- [14] L. Qu and W. Qiao, "Constant power control of DFIG wind turbines with super capacitor energy storage," IEEE Trans. Ind. Appl., vol. 47, no. 1, pp. 359-367, Jan./Feb. 2011.
- [15] G. Mandic, A. Nasiri, E. Ghotbi, and E. Muljadi, "Lithium-Ion capacitor energy storage integrated with variable speed wind turbines for power smoothing," IEEE J. Emerg. Sel. Topics Power Electron., vol. 1, no. 4, pp. 287–295, Dec. 2013.
- [16] R. Cardenas, R. Pena, G. Asher, and J. Clare, "Power smoothing in wind generation systems using a sensorless vector controlled induction Machine driving a flywheel," IEEE Trans. Energy Convers., vol. 19, no. 1, pp. 206-216, Mar. 2004.
- [17] S. Ghosh and S. Kamalasadan, "An energy function-based optimal control strategy for output stabilization of integrated DFIG-Flywheel energy storage system," IEEE Trans. on Smart Grid, vol. PP, no. 99, pp.1–10, to be published.
- [18] D. H. Doughty, P. C. Butler, A. A. Akhil, N. H. Clark, and J. D. Boyes, "Batteries for largescale stationary electrical energy storage," in Proc. Electrochem. Soc. Interface, Fall 2010, pp. 49–53.